AIAA Propulsion and Energy Forum
August 24-28, 2020, VIRTUAL EVENT
AIAA Propulsion and Energy 2020 Forum

10.2514/6.2020-3632

Impact of Flux Conservers on Performance of Inductively Driven Pulsed Plasmoid Thrusters

Christopher L. Sercel*, Joshua Woods †, Tate M. Gill‡, and Benjamin A. Jorns§
University of Michigan, Ann Arbor, MI, 48109

A general circuit model is developed to describe the operation of inductively-driven pulsed thrusters, including the introduction of an applied bias field and flux conservers. Equations of motion are solved using these circuit equations to arrive at maximum theoretical efficiency under conditions of instantaneous energy coupling into the plasma. It is found that flux conservers represent an inherent inductive efficiency loss in these devices. It is therefore concluded that flux conservers may be detrimental to the performance of pulsed thrusters whose primary acceleration mechanism is not thermal in nature.

Nomenclature

B_e = Magnetic field strength external to plasmoid separatrix
B_0 = Magnetic bias field strength prior to plasmoid formation
x_s = Ratio of plasmoid separatrix radius to flux conserver radius
F = Force
j = Current Density
L = Self-inductance
M = Mutual inductance
R = Resistance
I = Current
V = Voltage
C = Capacitance
u = Plasma bulk velocity
η = Efficiency
k = Mutual inductance geometric scaling parameter

Circuit Equation Subscripts

p = Plasma
b = Bias coil
d = Driver coil
ϕ = Flux conserver
ext = Refers to power circuit external to thruster body

I. Introduction

Pulsed electric propulsion schemes offer several alternative and highly enabling capabilities when compared with more traditional, steady-state concepts. For example, pulsed devices can, in principle, have nearly unlimited power throttling at a given thrust-to-power ratio. This capability could dramatically reduce typical mission complexity by

*PhD Candidate, Aerospace Engineering, 1320 Beal Ave, Ann Arbor, MI 48109, AIAA Student Member
†PhD Candidate, Aerospace Engineering, 1320 Beal Ave, Ann Arbor, MI 48109, AIAA Student Member
‡PhD Candidate, Aerospace Engineering, 1320 Beal Ave, Ann Arbor, MI 48109, AIAA Student Member
§PhD Candidate, Aerospace Engineering, 1320 Beal Ave, Ann Arbor, MI 48109, AIAA Senior Member

eliminating the need for separate thrusters for orbit changes versus station-keeping maneuvers. Similarly, using induction to couple power into the plasma eliminates the need for any plasma-wetted electrodes or screens, the erosion of which is a common failure point for traditional plasma propulsion systems. This allows the use of more exotic propellants than the typical xenon and krypton, such as water and carbon dioxide. These propellants can be found in space, possibly allowing for in-situ refuelling [1]. Inductively-driven thrusters are also uniquely suited to high power levels due to the tendency for thrust to scale quadratically, rather than linearly, with the current in the device [2]. In recent years, power is becoming increasingly available on-orbit due to advancements in solar panel technology [3], opening the field for very high power ($>$ 100 kW electric propulsion schemes and mission concepts (such as crewed transport). While there are on-going efforts to explore methods to scale more conventional EP technologies like Hall thrusters to access these power regimes, the non-linear power scaling of inductive thrusters makes them an alternative and highly attractive option.

While there are multiple concepts for high-power inductively pulsed thrusters, one concept that recently has received attention from both NASA and the Department of Defense is the Field-Reversed Configuration (FRC) thruster. Leveraging heritage from the fusion community [4], the FRC thruster is intended to form a confined plasmoid and accelerate this self-contained ball of plasma out of the device. Support from NASA and the defense community stems from several unique attributes of the FRC thruster in addition to those listed above. The confined nature of an FRC plasmoid means that no surfaces are plasma-wetted, eliminating erosion entirely as a failure mechanism and allowing for ISRU propellants such as direct use of extraterrestrial atmosphere [5][6]. It also eliminates any wall losses which would result in reduced efficiency. The geometry of the FRC has the potential for better coupling between the driver coil and the plasma itself because the conical nature of the driver coil allows the plasma to remain close throughout the acceleration process [7]. In addition to a theta-pinch type configuration [8], FRC thrusters can be operated using an RF wave in the r-θ plane, a configuration known as a Rotating Magnetic Field (RMF)-FRC [9]. This has the benefit of reducing the magnitude of the currents required to run the device, allowing for use of modern steady-state power switching which can simplify and reuce the weight of any power processing system [10].

Despite the apparent advantages offered by RMF-FRC thrusters, there are still several open questions about the performance of these devices. Indeed, to date, only indirect performance measurements have been performed, and these have shown poor results ($<$ 8% efficiency) [11]. Direct measurements, and a thorough understanding of the design parameter space, are necessary to improve performance. The University of Michigan has recently completed work on a first design iteration to make direct thrust and efficiency measurements, and to inform development of analytical models [12],[13]. Significant portions of design were inherited from devices from literature, including thruster size and shape, magnitude of magnetic fields, and the presence of what is known as a flux conserving surface outside the thruster cone, the last being the subject of this work.

To complement our efforts to explore thruster performance experimentally, there is also a need to revisit our understanding of the key principles of operation. For example, while the function of most of the components of FRC-thruster design are intuitive, e.g. the need for applied magnetic field and the configuration of the source for driving the inductive current, there is some ambiguity about the role of one key element in the design, the so-called flux conservers. Putatively, these components are a carry-over from the origins of FRCs as a mechanism for confining high energy density plasmas. In this capacity, they serve to increase the magnetic pressure within the device and therefore enhance heating and confinement. With that said, despite this function of improving confinement, it has been suggested that when implemented in a thruster configuration, these conservers can also can help facilitate movement of the plasma due to the conical, rather than cylindrical, shape of the magnetic field in a thruster rather than fusion device. This conical shape would cause the radial pressure balance between thermal pressure of the plasmoid and the augmented magnetic pressure to result in an unbalanced axial component [11]. This notable contrast from their original function (containment versus acceleration) invites the question as to how the flux conservers actually promote this acceleration. Indeed, intuitively, it might even be expected that the conservers actually hinder acceleration in the same way as a permanent magnet experiences a drag while falling through a conductive tube.

Although there have been a number of scaling laws that have been proposed for the performance of FRC thruster, to our knowledge, there has not been a detailed analysis to address the impact of the flux conservers on acceleration. For the purpose of establishing both an improved understanding and guiding future thruster design, there is an apparent need to revisit the role of these components from a first-principles analysis. To this end, we investigate in this work the impact of the flux conservers through an equivalent circuit analysis. In Section II, we review plasmoid thrusters and the current justification of the role of flux conververs. In Section III.A, we revisit the role of flux conservers through an equivalent circuit analysis. Finally, we draw conclusions regarding the validity of our analysis and proper design of these thrusters in Section IV.

II. Overview of Plasmoid Thruster Principles of Operation

In this section, we will give an overview of basic thruster operation.

Figure 1 shows the basic process of a pulse in a generic plasmoid thruster. First, a steady magnetic field is generated using magnets situated outside the thrust cone. This magnetic field, known as the bias field, must have both axial and radial components. At the beginning of the pulse, a pre-ionizer releases propellant with some seed ionization into the thrust cone. When this pre-ionized gas has filled the cone, the driver antenna induces an azimuthal current in the plasm. The plasmoid is formed when the resulting magnetic field is stronger than the axial component of the bias field near centerline, but weaker close to the wall. This creates a magnetic separatrix which confines the plasma and gives the Field-Reversed Configuration its name. The azimuthal current in the plasma can then interract with the radial component of the bias field via the Lorentz force to produce axial thrust. This clears the thrust cone of propellant, leaving it ready for the next pulse.

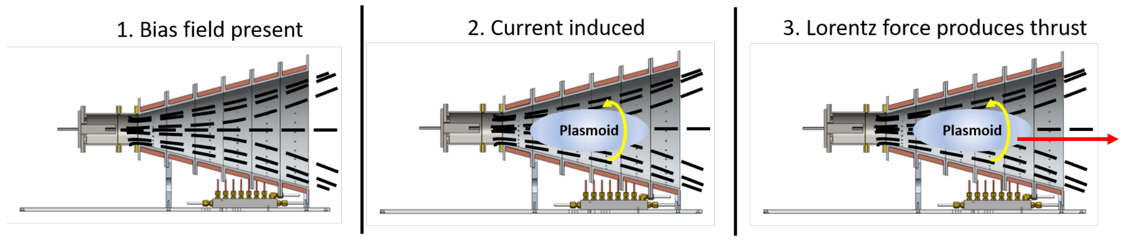

Fig. 1 The basic process of plasmoid acceleration. First the steady bias field is generated, then ionized gas is puffed in and current is induced for form the plasmoid. Finally, azimuthal currents in the plasmoid interract via the Lorentz force with the radial component of the bias field to produce thrust.

Several basic assumptions are encapsulated in Figure 1 and the preceding explanation. First, it is understood that we deal with a azimuthally-symmetric, conical plasma. This plasma fills the thrust cone and has a high degree of ionization due to the pre-ionizer. We also assume that the primary thrust mechanism is magnetic, rather than thermal in nature, as it results from the Lorentz force interaction between the bias coil and the plasma currents. In our scaling analysis presented in this study, we will ignore thermal effects. Finally, we have assumed that we are able to achieve plasmoid formation, which in reality requires careful tuning of operating parameters. This allows us to ignore effects such as field line detachment.

A. Current Drive

Fundamental to the operation of any inductively-driven pulsed thruster is a current drive mechanism which can couple energy into the plasma. This inductive current is a key component for accelerating the plasmoid. There are two general methods that have been explored for plasmoid thrusters: θ-pinch-like configurations (such as the Air Force, Michigan Tech, and UM's original work, the PTX) and rotating magnetic field (MSNW's ELF thruster). Figure 2 shows illustrations of both concepts.

In brief, the theta-pinch configuration works by placing a concentric conductor adjacent to the plasma. In the case of two conductors oriented similarly to each other, the result of driving a changing current in one loop is to produce an opposite changing current in the other, such that the secondary current mirrors the first. Throughout this work, we will refer to this type of current drive mechanism as the mirror current drive. At the most basic level, the mirror current drive will induce a current proportional to the time derivative of the original current. In contrast, the rotating magnetic field (RMF) works similarly to the operation of an induction motor. Antennas which form helmholtz pairs situated outside the thruster body are pulsed out of phase with each other. This produces a magnetic field oriented transverse to the cone or tube containing the plasma, and which appears to rotate azimuthally. Electrons, entrained by the magnetic field lines, then produce an azimuthal current opposite the rotation of the field. Because the electrons will rotate around the centerline of the device at the same frequency as the magnetic field, the induced current is not directly proportional to derivative of the current in the antennas as in the mirror drive, but rather its frequency.

B. The role of flux conservers in acceleration

Flux conservers are arrayed around the thruster concentrically to form surface, as in Figure 3, which resists any change in magnetic flux through its cross section. Typically consisting of thin rings of segmented metal, the addition of

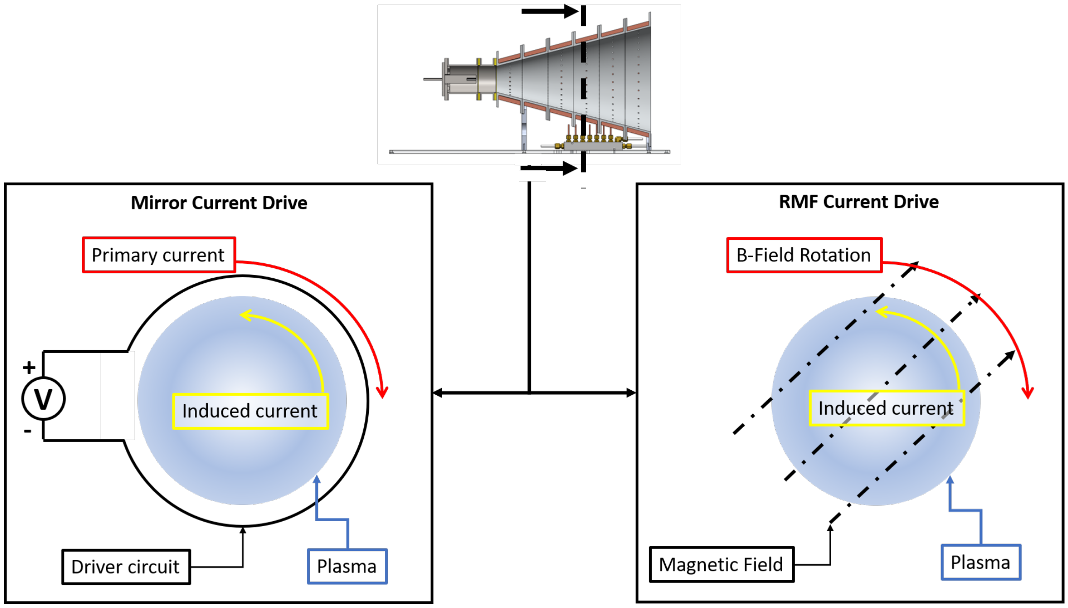

Fig. 2 The two spinup mechanisms identified for plasmoid thrusters. The mirror current drive induces a changing current opposite and proportional to that in a driver coil, while the RMF entrains electrons in a rotating magnetic field.

flux conservers to FRC thrusters is intended to maintain the total magnetic flux through the cone containing the plasma. Per previous work [14], it has been suggested that the flux conservers in FRC thrusters serve two roles: to help confine the plasmoid during initial FRC formation and to improve acceleration. We discuss both processes here.

Because FRC thrusters are designed to reverse the magnetic field inside the plasma though induction of strong aziumuthal currents, a separatrix is formed inside of which the net magnetic flux is zero. If the net flux is maintained, then the post-formation magnetic field between the separatrix and the wall must be stronger than the pre-formation field. This is described by the relation

$$B_e = \frac{B_0}{1 - x_s^2}, \tag{1}$$

where B_e is the field external to the separatrix, B_0 is the nominal bias field strength, and x_s is the ratio of the separatrix radius to the flux conserver radius [11]. Therefore the magnetic pressure outside the plasmoid, which scales as the square of the magnetic field, is significantly increased by the introduction of the flux conservers. It is argued that this serves to contain the plasma during FRC formation, preventing the leak of thermal energy to the walls. Indeed, for high-energy density experiments based on FRC plasmoids, flux conserver lossiness is a key figure of merit for the quality of the machine [15].

In contrast to previous energy experiments, however, where the goal typically is to confine the plasmoid, the plasmoid ultimately must be accelerated in thruster concepts. It has been suggested that flux conservers can also help facilitate this process. In particular, the acceleration of the RMF-FRC is an electromagnetic process [9] in which the driver is a Lorentz force given by

$$F_z = \int j_\theta B_r dV. \tag{2}$$

If the plasmoid is allowed to expand (increase in x_s) as it translates, the conservers act to maintain magnetic flux. Per Equation 1, this leads to an increase in the magnetic field at the periphery of the plasmoid several times larger than the initial applied field. This amplified B interacts with the current already circulating in the plasmoid leading to enhanced Lorentz acceleration, as can be seen in Figure 3. This process can be likened to a toothpaste tube like effect where the resistance of the plasmoid to expansion upstream leads to the expulsion of the FRC downstream. Absent the flux conservers, it is argued this type of amplified acceleration would not exist.

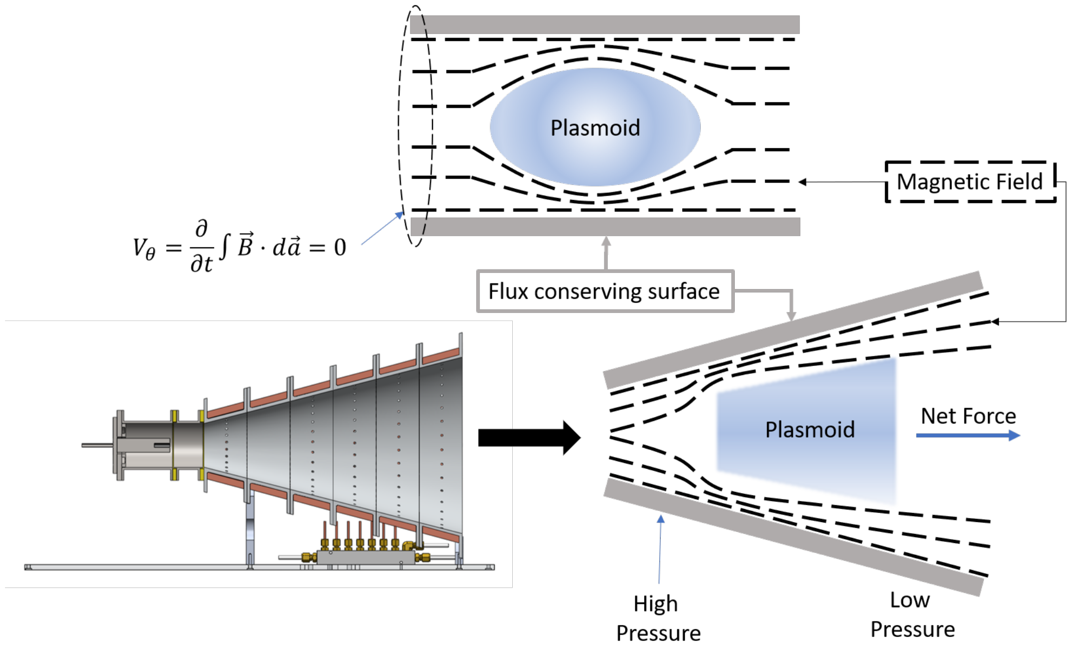

Fig. 3 In a traditional FRC confinement scheme, flux conservers are important for radial equilibrium by balancing thermal and magnetic pressure. It is argued that, by changing to a conical geometry, that pressure balance would net an axial force, akin to squeezing the toothpaste out of a tube

With that said, this description invites some questions about the physical validity of this proposed process. This can be illustrated with a simplified example. If a plasmoid is formed upstream of a flux conserver and then translates toward it, the flux conserver will induce a magnetic field to resist the change in flux. This could lead to a *slowing down* of the translating FRC to minimize the change in flux rather than an acceleration through the conserver, similar to the drag which acts on a magnet. This physical description contrasts the result shown in Fig. and invites a possible contradiction.

To attempt to resolve this apparent discrepancy, we consider in the next section a reduced fidelity circuit model for the plasmoid acceleration.

III. Equivalent Circuit Analysis of Plasmoid Thruster

In this section, we will introduce a reduced fidelity model for the interaction of the various thruster components. This will allow us to model currents in the plasma as well as the structural elements and arrive at the acceleration of the plasmoid. Subsequently applying assumptions such as energy conservation will then allow us to elucidate the role of the flux conservers by arriving at a final expression for the ideal efficiency of this device.

A. Formulation of equivalent circuit

To understand the plasmoid thruster, we employ circuit analysis, a powerful technique for modelling many electromechanical devices. It has been widely used in the pulsed electric propulsion community to describe thrusters such as the Pulsed Inductive Thruster [16] and the theta-pinch FRC thruster [17]. The general process is to abstract the device into separate current loops, each of which is representative of a component. By noting how driving a current through one loop impacts itself and the other loops, we can ascribe inductances, capacitances, and resistances to these loops. This leaves us with a time-dependent series of equations with several tuning parameters relating to the mutual inductances between the current loops.

For the purposes of this analysis, we will model a mirror current drive with flux conservers and a bias field. To facilitate this analysis, we make the following simplifications for the physical system shown in Figure 4 :

- We can denote a volume average azimuthal current denoted as plasma I_p
- There is a volume averaged current in the bias coils

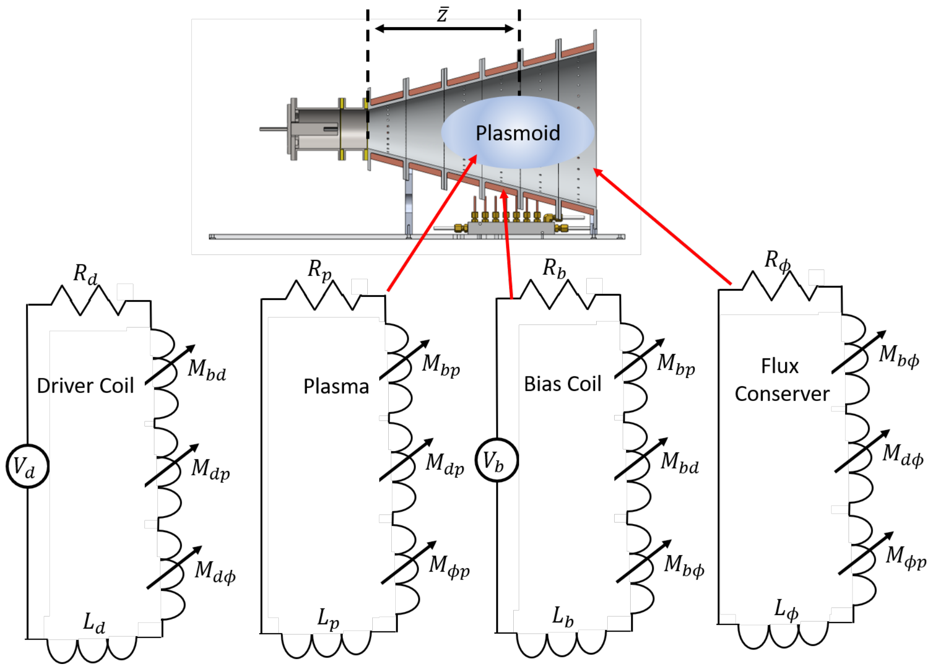

Fig. 4 Diagram of our circuit model with corresponding rendering of the thruster being developed by the University of Michigan. Driver coil not pictured here.

- We can denote the current in the drive circuit that induces current in the plasma as I_d. This is coupled via electromagnetic flux to the plasma

Subject to these assumptions and maintaining complete generality, we show in Appendix IX that this physical system can be represented with the equivalent circuit shown in Figure 4. The governing equations for this circuit in turn are given by

$$\frac{\partial}{\partial t}\left[L_p I_p + M_{d,p} I_d + M_{p,\phi} I_\phi + M_{b,p} I_b\right] + R_p I_p = 0 \tag{3}$$

$$V_d + \frac{\partial}{\partial t}\left[(L_d + L_{ext}) I_d + M_{d,p} I_p + M_{d,\phi} I_\phi + M_{b,d} I_b\right] + R_d I_d + \frac{1}{C_{ext}} \int I_d dt = 0 \tag{4}$$

$$\frac{\partial}{\partial t}\left[L_\phi I_\phi + M_{d,\phi} I_d + M_{p,\phi} I_p + M_{b,\phi} I_b\right] + R_\phi I_\phi = 0 \tag{5}$$

$$V_b + \frac{\partial}{\partial t}\left[L_b I_b + M_{b,d} I_d + M_{b,\phi} I_\phi + M_{b,p} I_p\right] + R_b I_b = 0, \tag{6}$$

where L refers to self inductance, M to mutual inductance, R to resistance, and V to voltage, and where the subscripts b, d, p, and ϕ refer to the bias coils, driver coils, plasma, and flux conservers, respectively. Each of these equations physically represents the voltage balance in a current loop, which must sum to zero for closed loops such as these. The first equation describes the plasma. Because the plasma itself has no direct voltage source, resistive losses and impedance due to self inductance must balance the EMF induced by the bias coil, driver coil, and flux conservers. Examining these terms in further detail, we note that taking the time derivative on the left-hand side will result in some terms with derivatives of inductances, and some terms with derivatives of currents. The changing-inductance terms represent a back-EMF resulting from relative motion between components, in the way that eddy currents develop when conductors are moved relative to magnets. The changing-current terms represent the back-EMF resulting from a mirror currents induced by current ramp-up in the same way a conductor tends to shield RF signal. The next equation, which describes the driver coil, has a similar form but adds the capacitance and inductance of the line to the power processing unit, as well as a voltage term, since it is actively driven. These are, in essence, generic Kirchoff's voltage loops for each individual component in the device.

It is critical to recognize the current convention used in the above equations. Because these equations are derived by examining current loops in real space, the current also follows real space conventions. Therefore, defining $\hat{\theta}$ in the typical way relative to the $\hat{z}$-direction in Figure 4, positive I corresponds to positive current flow in the positive $\hat{\theta}$-direction, and negative current flows in the negative $\hat{\theta}$-direction. Thus, driving an increasing current in one will result in a decreasing current in a nearby loop. This is ***opposite*** what is typically seen in a circuit diagram, in which a positive changing current induces a positive changing current. While this may be unusual to those accustomed to circuit equations in which self- and mutual inductance terms are on opposite sides of the equation, the advantage is that, in this system of four current loops, one can easily visualize in real space what is meant by a positive or negative current.

Note that all bias coils have been grouped into a single effective current loop, as with the driver coils and flux conservers. Notably, this result allows us to express the operation of the device in terms of lump parameters and circuit elements. Because many of these parameters are *ad hoc* in nature, the challenge lies in determining appropriate models for these lump circuit elements [17], but we can employ some simplifications to help facilitate the analysis. To this end, we enforce the following:

- Parasitic resistance and capacitance, as well as external inductances, are ignored. This idealizes the system somewhat, but should not have a major qualitative impact on behavior. Mathematically, this means $R_b = R_d = R_p = R_\phi = L_{ext}0$, and we ignore $\frac{1}{C_{ext}} \int I_d dt$.
- The self inductances of the bias coils, driver coils, and flux conservers, as well as the mutual inductances between the same, are constant due to their fixed geometry and the fact that all these quantities, by definition, are purely geometric in nature. Therefore $\dot{L}_{ext} = \dot{L}_b = \dot{L}_d = \dot{L}_\phi = \dot{M}_b = \dot{M}_d = \dot{M}_\phi = 0$
- The bias coils are driven with a current-controlled power supply, allowing us to treat the bias coil current as constant, so that $\dot{I}_b = 0$

Subject to these simplifications, Equations 3-6 become

$$\dot{L}_p I_p + L\dot{I}_p + \dot{M}_{d,p} I_d + M_{d,p}\dot{I}_d + \dot{M}_{p,\phi} I_\phi + M_{p,\phi}\dot{I}_\phi + \dot{M}_{b,p} I_b = 0 \tag{7}$$

$$V_d + L_d\dot{I}_d + \dot{M}_{d,p} I_p + M_{d,p}\dot{I}_p + M_{d,\phi}\dot{I}_\phi = 0 \tag{8}$$

$$L_\phi\dot{I}_\phi + M_{d,\phi}\dot{I}_d + \dot{M}_{p,\phi} I_p + M_{p,\phi}\dot{I}_p = 0 \tag{9}$$

$$V_b + M_{b,d}\dot{I}_d + M_{b,\phi}\dot{I}_\phi + \dot{M}_{b,p} I_p + M_{b,p}\dot{I}_p = 0 \tag{10}$$

The assumptions made above have several effects on the circuit equations. While the plasma circuit is largely unchanged except for a single resistive term, the stipulation that structural inductances be constant dramatically simplified the other equations. From a circuit perspective, this is equivalent to a requirement for fixed geometry. Meanwhile the third requirement breaks the reciprocity of these equations. It implies that energy must be added and removed from the system via the bias coil voltage to provide the constant current which produces the constant magnetic field. The physical relevance of these terms beyond what would describe a current ringdown is important when we consider that these circuit equations can be directly converted to a force equation for the plasma.

B. Acceleration model

We next use our circuit model to develop a force equation to describe the acceleration of the plasma itself. There are multiple routes for deriving this equation. It can be done using an ion momentum equation along with Ohm's Law to describe how the currents in the plasma react to the various fields present, but here we employ the work-force theorem, which states

$$\vec{F} = -\vec{\nabla} E\left(\vec{r}, t\right), \tag{11}$$

where F is the force and E is the energy of the object. In our case, the energy of a system of coupled inductors is given by

$$E_{mag} = \frac{1}{2} L_p I_p^2 + \frac{1}{2} L_d I_d^2 + \frac{1}{2} L_\phi I_\phi^2 + \frac{1}{2} L_b I_b^2 + M_{b,d} I_b I_d + M_{b,\phi} I_b I_\phi + M_{b,p} I_b I_p + M_{d,p} I_d I_p + M_{p,\phi} I_p I_\phi. \tag{12}$$

The four terms on the left represent the energy stored in each given current loop due to their own self-inductance, and the following terms represent the energy associated with their interactions. In other words, a self-inductive term such as $\frac{1}{2} L_d I_d^2$ represents the amount of energy which must be put into the driver coil in order to reach a current I_d absent any other conductive elements nearby. Meanwhile, the change in flux through a nearby bias boil associated with the increase in driver current from 0 to I_d will induce a back-EMF which would tend to drive an opposite current in the bias coil. Therefore, to maintain some I_b in the bias coil throughout the process of increasing driver current to I_d requires a greater amount of energy, with the difference given by $M_{d,p} I_d I_p$. Of course, the initial energy to build up the bias current must be accounted for. Also note that due to our circuit convention grounded in physical space rather than typical circuit diagram convention, the signs of the mutual inductive terms may be opposite to what the reader is accustomed to.

Next, we must take the spacial derivative of this equation to get the force. To do so, we must make an additional assumption: **the plasma has some centroid with a coordinate** z with time derivative $u = \frac{\partial \bar{z}}{\partial t}$ which we can call the bulk velocity of the plasma, as shown in Figure 4. If that is the case, then we can make a change of variables, for example:

$$\frac{\partial I}{\partial z} = \frac{1}{u} \frac{\partial I}{\partial z} \tag{13}$$

The result of taking the negative z derivative of Equation 12 can then be simplified by using Equations 7-10 to eliminate any derivatives of current. We then arrive at

$$F = m\dot{u} = \frac{1}{2} \frac{\partial L_p}{\partial \bar{z}} I_p^2 + \frac{\partial M_{b,p}}{\partial \bar{z}} I_b I_p + \frac{\partial M_{d,p}}{\partial \bar{z}} I_d I_p + \frac{\partial M_{p,\phi}}{\partial \bar{z}} I_p I_\phi + \frac{1}{u} V_d I_d, \tag{14}$$

where m is the mass of the plasmoid being accelerated, a quantity that is assumed to be constant. Next, using the same u as before to change variables, we can translate this force into a time rate of change of kinetic energy by multiplying both sides by u and rearranging:

$$m\dot{u}u = \frac{1}{2} \frac{\partial L_p}{\partial \bar{z}} I_p^2 u + \frac{\partial M_{b,p}}{\partial \bar{z}} I_b I_p u + \frac{\partial M_{d,p}}{\partial \bar{z}} I_d I_p u + \frac{\partial M_{p,\phi}}{\partial \bar{z}} I_p I_\phi u + V_d I_d \tag{15}$$

$$\frac{1}{2} m \frac{\partial}{\partial t} \left[u^2 \right] = \frac{1}{2} \dot{L}_p I_p^2 + \dot{M}_{b,p} I_b I_p + \dot{M}_{d,p} I_d I_p + \dot{M}_{p.\phi} I_p I_\phi + V_d I_d \tag{16}$$

Equation 16 relates the rate of change of kinetic energy of our plasma to the change in energy of the circuit elements. It is a remarkably simple result given the derivation. In the process of differentiating Equation 12, we have not blindly only performed the derivative on the mutual inductance terms, which would net the opposite result. We have used the chain rule on each term and solved the resulting equation using the system of circuit equations to arrive at this point. Therefore, although the we have expressed the change of kinetic energy in terms of the instantaneous currents, the way that those currents develop over time in this particular coupled inductive system is inherent to the result. The first term, $\frac{1}{2} \dot{L}_p I_p^2$, describes the trade-off between current and self-inductance which occurs in the plasma to minimize the potential energy in the plasma. Self-inductance, which is a function of the plasma's shape and will be greater for a larger, more expanded plasma, will increase as a function of $\bar{z}$. This term is strictly positive in this system and tells us that the plasma current acts as a source of energy to be used in acceleration. The mutual inductive terms describe the Lorentz force interaction between the plasma currents and whatever currents exist in those structural elements. Because mutual inductance between the plasma and the structural elements will decrease with $\bar{z}$, structure currents must be opposite to the plasma to add energy to the system. As discussed in Section III.A, driving a current in one loop will induce an opposite current in a secondary loop. As a sanity check, then, the driver coil indeed causes a net positive force.

We wish to use Equation 16 to arrive at some expression for the final bulk kinetic energy imparted to our plasma. To do so, we continue to substitute expressions from Equations 7-10 in an attempt to eliminate currents other than the plasma current. The result we arrive at is given by

$$\frac{\partial}{\partial t} \left[\frac{1}{2} m u^2 \right] = -\frac{\partial}{\partial t} \left[\frac{1}{2} \left(L_p - \left(\frac{M_{d,p}^2}{L_d} + \frac{M_{p,\phi}^2}{L_\phi} \right) \left(\frac{1}{1 - \frac{M_{d,\phi}^2}{L_d L_\phi}} \right) + 2 \frac{M_{d,p} M_{p,\phi} M_{d,\phi}}{L_d L_\phi - M_{d,\phi}^2} \right) I_p^2 \right] + \frac{M_{d,p}}{L_d} V_d I_p \tag{17}$$

This is a simplified energy conservation equation which frames the dynamics of the system as entirely as possible in terms of the plasma current. The first term on the right-hand side represents the loss of magnetic energy in the system, as we can identify it as the time rate of change of an inductance multiplied by the square of a current. Meanwhile, the second term represents the power being introduced to the system via the driver coil power supply, and it this energy transfer is throttled somewhat by the mutual inductance between the driver and flux conservers. Finally, we note that the bias coil does not make an appearance in Equation 17. Because of our idealized constant-current supply assumption, the bias coil converts magnetic energy in the plasma currents to kinetic energy rather than introducing new energy. Because this occurs at the expense of the plasma current, this effect is inherent to the shape of $I_p(t)$. With all things being equal, the presence of the bias coil will have the effect of creating a shorter more intense acceleration. Now that we have an energy conservation equation, we can integrate it to find the final kinetic energy of the plasmoid to gain an efficiency estimate.

C. Thruster efficiency

For the purposes of estimating the final kinetic energy of the plasma ejected from the thruster (and thereby efficiency), we make one final assumption that energy is coupled into the plasmoid instantaneously. We will refer to this in the following discussion as the instantaneous spin-up assumption. In other words, this assumption states that the plasmoid forms in one step, then is accelerated in another step, with no additional energy coupled into the plasma from the driver during the acceleration process. This is implicit in the explanation of how a plasmoid thruster operates as discussed in Section II. However, although it is a common assumption in the analysis of these thrusters to ignore the plasmoid formation, it remains to be seen how correct this is in reality. Because the energy coupling happens initially and then stops, we can treat V_d as 0 for the duration of the pulse. This eliminates the final term on the right-hand side of Equation 17:

$$\frac{\partial}{\partial t}\left[\frac{1}{2}mu^2\right] = -\frac{\partial}{\partial t}\left[\frac{1}{2}\left(L_p - \left(\frac{M_{d,p}^2}{L_d} + \frac{M_{p,\phi}^2}{L_\phi}\right)\left(\frac{1}{1-\frac{M_{d,\phi}^2}{L_d L_\phi}}\right) + 2\frac{M_{d,p}M_{p,\phi}M_{d,\phi}}{L_d L_\phi - M_{d,\phi}^2}\right)I_p^2\right]. \tag{18}$$

This is a remarkable, non-path-dependent result which can then be integrated over time. We take the boundary conditions that $u(0) = 0$ and $I(t_f) = 0$ to indicate that all magnetic energy has been removed in the plasma, which is an idealized case. In that case,

$$\frac{1}{2}mu_f^2 = \frac{1}{2}L_p(0)I_p^2(0) - \frac{1}{2}\left(\frac{M_{d,p}^2(0)}{L_d(0)} + \frac{M_{p,\phi}^2(0)}{L_\phi(0)}\right)\left(\frac{1}{1-\frac{M_{d,\phi}^2(0)}{L_d(0)L_\phi}(0)}\right)I_p^2(0) + \frac{M_{d,p}(0)M_{p,\phi}(0)M_{d,\phi}(0)}{L_d(0)L_\phi(0) - M_{d,\phi}^2(0)}I_p^2(0) \tag{19}$$

We then note that the first term on the right hand side, $\frac{1}{2}L_p(0)I_p^2(0)$, represents the magnetic energy stored in the form of plasma current just after spin-up. In other words, this is the reservoir of energy from which the plasma accelerates. The next term refers to the magnetic energy which is coupled *back* into the driver coil and flux conservers, respectively, as a result of their mutual inductance, relative motion, and changing plasma current. The energy that is coupled back into the structure in this way is scaled down by the mutual inductance of the structural elements with each other, $M_{d,\phi}$, because that mutual inductance will tend to prevent these two elements from experiencing changing currents in the same direction. Finally, the third term represents a mechanism for energy to move back into the plasma after having been coupled into one structural element by passing through the other structural element. We can help illustrate this interpretation by eliminating the mutual inductance between the driver coil and the flux conservers. This would mean that the plasma can couple to each one independently, but energy could not pass directly from the flux conservers to the plasma. With this requirement, we have

$$\frac{1}{2}mu_f^2 = \frac{1}{2}L_p(0)I_p^2(0) - \frac{1}{2}\left(\frac{M_{d,p}^2(0)}{L_d(0)} + \frac{M_{p,\phi}^2(0)}{L_\phi(0)}\right)I_p^2(0), \tag{20}$$

in which the reduction in coupling back to the structure is eliminated, as is the path for energy to pass from one structure through another to the plasma. In any case, a bound on efficiency can be calculated using

$$\eta = \frac{\text{Final Kinetic Energy}}{\text{Input Magnetic Energy}} \tag{21}$$

$$= \frac{\frac{1}{2}mu_f^2}{\frac{1}{2}L_p(0)I_p^2(0)} \tag{22}$$

$$= 1 - \left(\frac{M_{d,p}^2(0)}{L_d(0)L_p(0)} - \frac{M_{p,\phi}^2(0)}{L_\phi(0)L_p(0)}\right)\left(\frac{1}{1 - \frac{M_{d,\phi}^2(0)}{L_d(0)L_\phi}(0)}\right) + \frac{2M_{d,p}(0)M_{p,\phi}(0)M_{d,\phi}(0)}{L_d(0)L_\phi(0)L_p(0) - L_p(0)M_{d,\phi}^2} \tag{23}$$

Then, because mutual inductances are commonly modelled as $M_{1,2} = k_{1,2}\sqrt{L_1 L_2}$, with k being a function of geometry and relative positioning [17], we can further simplify to

$$\eta = 1 - \frac{k_{d,p}^2(0) + k_{p,\phi}^2(0) + 2k_{d,p}(0)k_{p,\phi}(0)k_{d,\phi}(0)}{1 - k_{d,\phi}^2(0)}. \tag{24}$$

This expression describes the maximum possible thruster efficiency purely in terms of the coupling coefficients at initial plasma spinup. k is only a function of the relative position and orientation of the circuits whose coupling it describes, with a larger value corresponding to two physically close, similarly oriented circuits. In general, k has a maximum value approaching 1, and the values of the various k in a system cannot be independently arbitrarily adjusted. This eliminates the singularity as $k_{d,\phi} \to 1$ since that would require $k_{d,p} \to 0$ and $k_p, \phi \to 0$.

IV. Discussion

V. Physical implications of result

From Equations 24 and 27 we can make the conclusion that the presence of structural elements after the plasma has been spun up is detrimental to thruster performance. Maximizing the efficiency according to Equation 24 requires $k_{d,p} = k_{p,\phi} = kd, \phi = 0$. This is because the plasma will couple energy back into these structures, effectively leaving some portion of energy behind in the form of induced currents as it accelerates away. In the case of the driver coil, this conclusion is only valid in the instant spin-up case, because in the more realistic event of finite spin-up, the direction of energy transfer is always from the coil to the plasma, rather than the other way around. However, it is the entire purpose of the flux conservers to couple to the plasma, else they would not function to maintain constant flux even during plasma spin-up. In essence, we can compare the process of the plasma moving through the flux conservers to dropping a permanent magnet down a conductive tube. The tube serves to resist the motion of the magnet and reduce its kinetic energy. Therefore, the ultimate conclusion of this work is that, unless the goal is to design a thruster which relies primarily on thermal effects to produce thrust, flux conservers are detrimental and should not by employed.

This result is contrary to previous understanding of the role of flux conservers in plasmoid thrusters, which place them in a positive role due to their amplification of the magnetic field outside the separatrix radius. This model, which relies on the external magnetic field squeezing the plasmoid out of the thruster akin to a tube of toothpaste, clearly breaks down under the assumptions made here. One explanation is that the increased field strength due to the flux conservers occurs in a region in which the plasma current is zero since it is outside the separatrix radius. Thus, its impact on acceleration is ineffectual. Alternately, the 'toothpaste tube' model commonly assumes that the currents present in both the plasma and the flux conservers are constant, while in this model, currents decrease over time as energy is converted from magnetic to kinetic.

VI. Limitations of Analysis

It is critical to recognize the conditions under which the above analysis is valid. Revisiting the assumptions required to reach our final result, some are more realistic than others. In particular, the stipulation that the structural elements present (driver coil, bias coils, flux conservers) have constant inductances is very likely true. As inductance is a function of geometry, and these elements are fixed in space and in shape, there is no reason to expect their inductances, self or mutual, to change. The requirement that the plasma have some trackable centroid coorddinate is also likely reasonable. Not that this is not a slug assumption; the plasma is free to change shape over time. If this is not valid, the circuit equations cannot be solved in closed form for such a clean expression of total force;, however, major conclusions are unlikely to change. The constant-current power supply for the bias coils is also likely reasonable to assume. Further, in an experimental setting, this assumption can be tested by placing a current measurement on the line up to the bias coils, ensuring that the time resolution of such a measurement be faster than the plasmoid spin-up timescale. If it is found that the current does indeed change, the impact can be mitigated by placing an inductance in series with the bias coil to help resist any change in current.

Our requirement that resistances and other parasitic elements be negligible, while unlikely to be true, at least has a manageable impact. Increased parasitic effects will cause losses, limiting efficiency. Another loss that we have ignored as part of this analysis is the coupling between structural elements, especially the lack of coupling of the driver coil to the flux conservers and bias coils. Since these structures are all in close proximity since they must each be able to independently couple to the plasma, it is a near guarantee they will couple to each other. As a result, significantly less energy will move from the driver coil to the plasma, since the same total input will be split between that which is coupled to the plasma, flux conservers, and bias coil. Thus, this assumption is highly generous to the presence of flux conservers and bias coil.

While the above reasons for invalidating this analysis are possible, perhaps the most critical condition to verify is the time over which power is deposited into the plasma relative to its residency time nearby these structural elements. This instantaneous spin-up assumption eliminates the last term in Equation 18 which is helpful to the acceleration of the plasma it allows further energy to be introduced. Indeed, if we compare the current scaling of our result to verified analyses of other thrusters from the literature, there is strong evidence to suggest that this is not the case. Mikellides and Neilly (2004) [16] show that the final energy of the plasma in a Pulsed Inductive Thruster should be proportional to the fourth power of the current ($E_f = I_p^4$), while we show that it goes as the square. Given the generality of our analysis, we can match the PIT geometry simply by eliminating the bias field and the flux conservers, leaving us with

$$\frac{1}{2}mu_f^2 = \frac{1}{2}\left(L_p(0) - \frac{M_{d,p}^2(0)}{L_d(0)}\right)I_p^2(0) \tag{25}$$

Further, the PIT analysis does not take into account thermal effects or other major physics left out here. The only assumption we have made which could possibly result in superior scaling is the instant spin-up assumption. It is plausible to conclude, then, that the scaling found for the PIT is due to this effect. Intuitively, this is reasonable since finite spin-up means that energy will be converted to kinetic throughout the process. Therefore, the energy which must be coupled into the plasma to achieve a given current would be greater.

Next, we can consider that this analysis, after the instant spin-up assumption, is valid for not just mirror current drives, but RMF drives as well. While the details of the current generation process are different, the result post-coupling is the same - a plasma with an azimuthal current. The major difference would be that, due to the geometry of RMF antennas being axial rather than azimuthal in nature, it would be difficult for an azimuthal plasma current to directly couple back into the antenna. Therefore, all that is necessary to more closely resemble the effect of this assumption on the RMF drive is to eliminate $M_{d,p}$ from Equation 19, yielding:

$$\frac{1}{2}mu_{f,RMF}^2 = \frac{1}{2}\left(L_p(0) - \frac{M_{p,\phi}^2(0)}{L_\phi(0)}\right)I_p^2(0), \tag{26}$$

and thus

$$\eta_{RMF} = 1 - k_{\phi,p}^2(0). \tag{27}$$

In this system, we note that because only one mutual inductance is present, we are fundamentally free to adjust $k_{\phi,p}$ as we wish between 0 and 1. This, of course, gives us efficiency in the same bounds, which is expected.

VII. Conclusions

In this study, we sought to examine the impact of flux conservers, which are important components in a field-reversed configuration containment scheme, on the performance of plasmoid thrusters. To this end, we developed and applied a circuit model to these thrusters. Seeking an expression for efficiency, we applied idealized assumptions to the model, most notably the idea that energy be transfered from the driver coil to the plasma instantaneously. By enforcing these assumptions and solving the system, we found that flux conservers represent an inherent efficiency loss. It is unavoidable that energy from the plasma remain in the flux conservers in the form of induced current, limiting that which is available for acceleration. We have also discussed the situations in which our asssumptions are not likely to hold, and the possible consequences of their breakdown.

VIII. Acknowledgements

This work has been supported by NSTRF Grant #80NSSC18K1190. In addition, we would like to acknowledge Dr. Kurt Polzin for his insightful critiques, as well as Shadrach Hepner for fruitful discussions.

IX. Appendix: Circuit Equations Verification

We wish to rigorously verify that a circuit model is appropriate for a mirror current drive inductive device. To do so, we will derive the back-EMF on each component due to current in the other components to establish mutual inductances. We assume that each individual component has a well-understood self-inductance.

A. Driver Coil

Ampere's Law relates the curl of the electric field in the coil current loop to the local change in magnetic field:

$$\nabla \times \vec{E} = -\frac{\partial \vec{B}}{\partial t}. \tag{28}$$

Integrate this relation over the cross-sectional area of the coil loop C_n:

$$\int_{a_C} \left(\nabla \times \vec{E}\right) \cdot \hat{z} da = -\frac{\partial}{\partial t} \int_{a_C} \vec{B} \cdot \hat{z} da \tag{29}$$

$$V_n = 2\pi r_n E_{(\theta)}(\vec{r}_n) = -\frac{\partial}{\partial t} \int_{a_n} \vec{B} \cdot \hat{z} da, \tag{30}$$

where we have assumed axisymmetry, da denotes the differential area, $E_\theta(\vec{r}_n)$ is the electric field in the azimuthal direction along the coil loop, and r_n denotes the radius of the current loop. The left hand side represents the back EMF, V_n, along the loop induced by the change in magnetic flux through the loop (the right hand side). There are two contributions to the magnetic field in the loop: the field from the coil's own magnetic field, $\vec{B}_{C_n}$ and the field generated from the plasma slug, $\vec{B}_S$. If we consider the former, we would arrive at an expression related to L_C, the self-inductance of the coil. We have already represented this unambiguously as an equivalent circuit element. To calculate the flux contribution from the plasma slug, we invoke the concept of magnetic vector potential, $\nabla \times \vec{A} = \vec{B}$. Substituting into Equation 30, we find

$$\int_{a_n} \vec{B} \cdot \hat{z} da = \int_{a_n} \left(\nabla \times \vec{A}\right) \cdot \hat{z} da = 2\pi r_n \left(A_{b,\theta}(\vec{r}_n) + A_{p,\theta}(\vec{r}_n) + A_{\phi,\theta}(\vec{r}_n)\right), \tag{31}$$

where $A_{b,\theta}(\vec{r}_n)$ denotes the azimuthal component of the magnetic potential vector from the bias coils at the coil loop (located at spatial location of the coil, $\vec{r}_n$), $A_{p,\theta}(\vec{r}_n)$ represents that from the plasma, and $A_{\phi,\theta}(\vec{r}_n)$ is that from the flux conservers.

From Biot-Savart, we can relate the magnetic potential vector from the plasma current loop to the local current density in the slug:

$$A_{p,\theta}(\vec{r}_n) = \frac{\mu_0}{4\pi} \int \frac{j_{e(\theta)}(\vec{r}\,')}{|\vec{r}_n - \vec{r}\,'|} dV', \tag{32}$$

where the volume integral is over the entire measurement domain where the plasma can translate. We then make the assumption that we can write the azimuthal current density in the plasma as the product of the total azimuthal current, I_p, and a cros-sectional density weight factor $g_p(\vec{r}\,')$, such that $j_{e,\theta}(\vec{r}\,') = I_p g_p(\vec{r}\,')$ Therefore, the vector potential due to plasma current is

$$A_{p,\theta}(\vec{r}_n) = \frac{\mu_0 I_p}{4\pi} \int \frac{g_p(\vec{r}')}{|\vec{r}_n - \vec{r}'|} dV', \tag{33}$$

Next, the vector potential from the kth bias coil is

$$A_{b_k,\theta} = \frac{\mu_0 I_{b_k}}{4\pi} \oint_{b_k} \frac{d\vec{l}'_k}{|\vec{r}_n - \vec{r}'_k|} = \frac{\mu_0 I_{b_k} r_k}{4\pi} \oint_{b_k} \frac{d\theta'}{|\vec{r}_n - \vec{r}'_k|}, \tag{34}$$

and that from the mth flux conserver is

$$A_{\phi_m,\theta} = \frac{\mu_0 I_{\phi_m}}{4\pi} \oint_{\phi_m} \frac{d\vec{l}'_m}{|\vec{r}_n - \vec{r}'_m|} = \frac{\mu_0 I_{\phi_k} r_m}{4\pi} \oint_{\phi_m} \frac{d\theta'}{|\vec{r}_n - \vec{r}'_m|}. \tag{35}$$

We thus find for the voltage induced along the n^{th} coil of the driver loop:

$$\begin{aligned} V_{d_n} = -\frac{\partial}{\partial t}\Bigg[I_p \frac{\mu_0 r_n}{2} \oint_{d_n} \int \frac{g_p(\vec{r}')}{|\vec{r}_n - \vec{r}'|} dV' d\theta'' + I_b \sum_k^K \frac{\mu_0 g_{b_k} r_k r_n}{2} \oint_{d_n} \oint_{b_k} \frac{d\theta'}{|\vec{r}_n - \vec{r}'_k|} d\theta'' \\ + I_\phi \sum_m^M \frac{\mu_0 g_{\phi_m} r_m r_n}{2} \oint_{d_n} \oint_{\phi_m} \frac{d\theta'}{|\vec{r}_n - \vec{r}'_m|} d\theta'', \end{aligned} \tag{36}$$

where we have summed over each of K bias coils and M flux conservers. Similarly to the plasma, we have assumed that we can represent the current in each individual loop as the product of a constant total current and a weight factor. This is the back-emf induced in one loop of the inductor coil by the other components. If there are N turns, then

$$\begin{aligned} V_d = -\frac{\partial}{\partial t}\Bigg[I_p \sum_n^N \frac{\mu_0 r_n}{2} \oint_{d_n} \int \frac{g_p(\vec{r}')}{|\vec{r}_n - \vec{r}'|} dV' d\theta'' + I_b \sum_n^N \sum_k^K \frac{\mu_0 g_{b_k} r_k r_n}{2} \oint_{d_n} \oint_{b_k} \frac{d\theta'}{|\vec{r}_n - \vec{r}'_k|} d\theta'' \\ + I_\phi \sum_n^N \sum_m^M \frac{\mu_0 g_{\phi_m} r_m r_n}{2} \oint_{d_n} \oint_{\phi_m} \frac{d\theta'}{|\vec{r}_n - \vec{r}'_m|} d\theta'', \end{aligned} \tag{37}$$

B. Flux Conservers

We take a similar approach for the flux conservers. External sources of magnetic vector potential now include the plasma, bias coils, and driver coil. Contribution from the plasma is given again by the Biot-Savart Law as

$$A_{p,\theta}(\vec{r}_m) = \frac{\mu_0 I_p}{4\pi} \int \frac{g_p(\vec{r}')}{|\vec{r}_m - \vec{r}'|} dV', \tag{38}$$

where the subscript m refers to the mth flux conserving loop. Similarly, the bias coil contribution will be given by

$$A_{b,\theta} = \sum_k^K \frac{\mu_0 I_{b_k}}{4\pi} \oint_{b_k} \frac{d\vec{l}'_k}{|\vec{r}_m - \vec{r}'_k|} = \sum_k^K \frac{\mu_0 I_{b_k} r_k}{4\pi} \oint_{b_k} \frac{d\theta'}{|\vec{r}_m - \vec{r}'_k|}. \tag{39}$$

And for the driver coil:

$$A_{d,\theta} = \sum_n^N \frac{\mu_0 I_{d_n}}{4\pi} \oint_{d_n} \frac{d\vec{l}'_n}{|\vec{r}_m - \vec{r}'_n|} = \sum_n^N \frac{\mu_0 I_{d_n} r_n}{4\pi} \oint_{d_n} \frac{d\theta'}{|\vec{r}_m - \vec{r}'_n|}. \tag{40}$$

Since Equation 30 is still valid, we can then arrive at the total voltage on a flux conserving ring:

$$V_{\phi_m} = -\frac{\partial}{\partial t}\left[I_p \frac{\mu_0 r_m}{2}\oint_{\phi_m}\int \frac{g_p(\vec{r}')}{|\vec{r}_n - \vec{r}'|}dV' d\theta'' + I_b \sum_k^K \frac{\mu_0 g_{b_k} r_k r_m}{2}\oint_{\phi_m}\oint_{b_k}\frac{d\theta'}{|\vec{r}_m - \vec{r'}_k|}d\theta'' \right. \\ \left. + I_d \sum_n^N \frac{\mu_0 g_{d_n} r_n r_m}{2}\oint_{\phi_m}\oint_{d_k}\frac{d\theta'}{|\vec{r}_m - \vec{r'}_n|}d\theta''. \right] \tag{41}$$

Fundamentally, there is no requirement that flux conservers be connected end-to-end to form a single effective current loop, and each separate flux conserver would add its own equation to the system. However, we can make the system of equations significantly more manageable while only reducing generality a small degree by assuming they are. In that case we can sum over the individual loops to reach a total voltage:

$$V_{\phi} = -\frac{\partial}{\partial t}\left[I_p \sum_m^M \frac{\mu_0 r_m}{2}\oint_{\phi_m}\int \frac{g_p(\vec{r}')}{|\vec{r}_n - \vec{r}'|}dV' d\theta'' + I_b \sum_m^M \sum_k^K \frac{\mu_0 g_{b_k} r_k r_m}{2}\oint_{\phi_m}\oint_{b_k}\frac{d\theta'}{|\vec{r}_m - \vec{r'}_k|}d\theta'' \right. \\ \left. + I_d \sum_m^M \sum_n^N \frac{\mu_0 g_{d_n} r_n r_m}{2}\oint_{\phi_m}\oint_{d_k}\frac{d\theta'}{|\vec{r}_m - \vec{r'}_n|}d\theta''. \right] \tag{42}$$

Note that the last term on the right hand side exists in both the flux conserver and the driver coil equations with the current being that of the opposite element. We can recognize this as a mutual inductance, such that

$$M_{d,\phi} = \sum_m^M \sum_n^N \frac{\mu_0 g_{d_n} r_n r_m}{2}\oint_{\phi_m}\oint_{d_k}\frac{d\theta'}{|\vec{r}_m - \vec{r'}_n|}d\theta''. \tag{43}$$

C. Bias Coil

Again, we use the same process. The following equations represent the magnetic vector potential on the kth bias coil due to the plasma, the driver coil, and the flux conservers, respectively.

$$A_{p,\theta} = \frac{\mu_0 I_p}{4\pi}\int \frac{g_p(\vec{r}')}{|\vec{r}_k - \vec{r}'|}dV' \tag{44}$$

$$A_{d,\theta} = \sum_n^N \frac{\mu_0 I_{d_n}}{4\pi}\oint_{d_n}\frac{d\vec{l}'_n}{|\vec{r}_k - \vec{r'}_n|} = \sum_n^N \frac{\mu_0 I_{d_n} r_n}{4\pi}\oint_{d_n}\frac{d\theta'}{|\vec{r}_k - \vec{r'}_n|} \tag{45}$$

$$A_{\phi,\theta} = \sum_m^M \frac{\mu_0 I_{\phi_m}}{4\pi}\oint_{\phi_m}\frac{d\vec{l}'_m}{|\vec{r}_k - \vec{r'}_m|} = \sum_m^M \frac{\mu_0 I_{\phi_m} r_m}{4\pi}\oint_{\phi_m}\frac{d\theta'}{|\vec{r}_k - \vec{r'}_m|}, \tag{46}$$

yielding the total voltage

$$V_b = -\frac{\partial}{\partial t}\left[I_p \sum_k^K \frac{\mu_0 r_k}{2}\oint_{b_k}\int \frac{g_p(\vec{r}')}{|\vec{r}_k - \vec{r}'|}dV' d\theta'' + I_d \sum_n^N \sum_k^K \frac{\mu_0 g_{d_n} r_n r_k}{2}\oint_{b_k}\oint_{d_n}\frac{d\theta'}{|\vec{r}_k - \vec{r'}_n|} \right. \\ \left. + I_\phi \sum_m^M \sum_k^K \frac{\mu_0 g_{\phi_m} r_m r_k}{2}\oint_{b_k}\oint_{\phi_m}\frac{d\theta'}{|\vec{r}_k - \vec{r'}_m|}. \right] \tag{47}$$

This allows us to again recognize shared terms:

$$M_{b,\phi} = \sum_{m}^{M}\sum_{k}^{K}\frac{\mu_0 g_{\phi_m} r_m r_k}{2}\oint_{d_k}\frac{d\theta'}{|\vec{r}_k - \vec{r'}_m|} \tag{48}$$

$$M_{b,d} = \sum_{n}^{N}\sum_{k}^{K}\frac{\mu_0 g_{d_n} r_n r_k}{2}\oint_{b_k}\frac{d\theta'}{|\vec{r}_k - \vec{r'}_n|} \tag{49}$$

D. Plasma Circuit

We use a generalized Ohm's Law for the electron dynamics in the plasma circuit:

$$\vec{E} - \frac{\vec{j}_e}{n_e q}\times\vec{B} = \eta\vec{j}_e, \tag{50}$$

where we include local resistivity, but not thermal/pressure effects. We take the curl of Equation 50 and employ Ampere's Law to express everything in terms of magnetic fields:

$$-\frac{\partial\vec{B}}{\partial t} - \nabla\times\left(\frac{\vec{j}_e}{n_e q}\times\vec{B}\right) = \nabla\times\left(\eta\vec{j}_e\right). \tag{51}$$

This relationship shows that the flux from the changing magnetic field must be balanced by currents in the plasma. We now integrate over a current loop C' of constant radius r' in the plasma.

$$-\frac{\partial}{\partial t}\int_{a_{C'}}\vec{B}\cdot\hat{z}da' - \int_{a_{C'}}\left(\nabla\times\left(\frac{\vec{j}_e}{n_e q}\times\vec{B}\right)da'\right)\cdot\hat{z}da' = \int_{a_{C'}}\left(\nabla\times\left(\eta\vec{j}_e\right)\right)\cdot\hat{z}da'. \tag{52}$$

Again, we use the magnetic vector potential and apply Stokes' theorem to change these area integrals to contour integrals.

$$-\frac{\partial}{\partial t}\left[2\pi r'\left(A_{p,\theta}(\vec{r}') + A_{b,\theta}(\vec{r}') + A_{d,\theta}(\vec{r}') + A_{\phi,\theta}(\vec{r}')\right)\right] - 2\pi r'\left(\frac{\vec{j}_e}{n_e q}\times\vec{B}\right)\cdot\hat{\theta} = 2\pi r'\eta(\vec{r}')j_{e(\theta)}(\vec{r}'), \tag{53}$$

where we have assumed axisymmetry to perform the line integrals. We have also broken up the magnetic vector potential into the external contributions: the plasma itself, and the bias, driver, and flux conserver current loops. To further simplify, we assume that the electron current density in the plasma is only in the azimuthal direction so that we can eliminate the second term, to arrive at

$$-\frac{\partial}{\partial t}\left[2\pi r'\left(A_{p,\theta}(\vec{r}') + A_{b,\theta}(\vec{r}') + A_{d,\theta}(\vec{r}') + A_{\phi,\theta}(\vec{r}')\right)\right] = 2\pi r'\eta(\vec{r}')j_{e(\theta)}(\vec{r}'). \tag{54}$$

Those contributions at a given location are again

$$A_{p,\theta} = \frac{\mu_0 I_p}{4\pi}\int\frac{g_p(\vec{r}')}{|\vec{r}-\vec{r}'|}dV' \tag{55}$$

$$A_{b,\theta} = \sum_{k}^{K}\frac{\mu_0 I_{b_k}}{4\pi}\oint_{b_k}\frac{d\vec{l}'_k}{|\vec{r}-\vec{r'}_k|} = \sum_{k}^{K}\frac{\mu_0 I_{b_k} r_k}{4\pi}\oint_{b_k}\frac{d\theta'}{|\vec{r}-\vec{r'}_k|} \tag{56}$$

$$A_{d,\theta} = \sum_{n}^{N}\frac{\mu_0 I_{d_n}}{4\pi}\oint_{d_n}\frac{d\vec{l}'_n}{|\vec{r}-\vec{r'}_n|} = \sum_{n}^{N}\frac{\mu_0 I_{d_n} r_n}{4\pi}\oint_{d_n}\frac{d\theta'}{|\vec{r}-\vec{r'}_n|} \tag{57}$$

$$A_{\phi,\theta} = \sum_{m}^{M}\frac{\mu_0 I_{\phi_m}}{4\pi}\oint_{\phi_m}\frac{d\vec{l}'_m}{|\vec{r}-\vec{r'}_m|} = \sum_{m}^{M}\frac{\mu_0 I_{\phi_m} r_m}{4\pi}\oint_{\phi_m}\frac{d\theta'}{|\vec{r}-\vec{r'}_m|} \tag{58}$$

Next, we can multiply Equation 54 by the same plasma current weight factor, g_p, and integrate throughout the volume of the thruster (using the double prime notation to refer to this integral):

$$-\frac{\partial}{\partial t}\left[I_p \iint \left(\frac{\mu_0}{4\pi}\frac{g(\vec{r}')g(\vec{r}'')}{|\vec{r}'-\vec{r}''|}dV''dV'\right) + I_b \sum_k^K \frac{\mu_0 r_k}{2}\oint_{b_k}\int \frac{g_p(\vec{r}')}{|\vec{r}_k-\vec{r}'|}dV'd\theta'' + I_d \sum_n^N \frac{\mu_0 r_n}{2}\oint_{d_n}\int \frac{g_p(\vec{r}')}{|\vec{r}_n-\vec{r}'|}dV'd\theta'' \right.$$
$$\left. + I_\phi \sum_m^M \frac{\mu_0 r_m}{2}\oint_{\phi_m}\int \frac{g_p(\vec{r}')}{|\vec{r}_n-\vec{r}'|}dV'd\theta'' = I_p \int (g(\vec{r}'))^2 \eta(\vec{r}')dV' \right. \tag{59}$$

Once again, we recognize shared terms to identify the forms of the mutual inductances:

$$M_{b,p} = \sum_k^K \frac{\mu_0 r_k}{2}\oint_{b_k}\int \frac{g_p(\vec{r}')}{|\vec{r}_k-\vec{r}'|}dV'd\theta'' \tag{60}$$

$$M_{d,p} = \sum_n^N \frac{\mu_0 r_n}{2}\oint_{d_n}\int \frac{g_p(\vec{r}')}{|\vec{r}_n-\vec{r}'|}dV'd\theta'' \tag{61}$$

$$M_{p,\phi} = \sum_m^M \frac{\mu_0 r_m}{2}\oint_{\phi_m}\int \frac{g_p(\vec{r}')}{|\vec{r}_n-\vec{r}'|}dV'd\theta'' \tag{62}$$

Additionally, from the plasma circuit we have derived the self-inductance and resistance as

$$L_p = \iint \frac{\mu_0}{4\pi}\frac{g(\vec{r}')g(\vec{r}'')}{|\vec{r}'-\vec{r}''|}dV''dV' \tag{63}$$

$$R_p = \int (g(\vec{r}'))^2 \eta(\vec{r}')dV'. \tag{64}$$

Thus, we have identified the mutual inductances which dictate the six total coupling paths for this system of four current loops.

References

[1] Mahoney, E., "In-Situ Resource Utilization," 2018. URL `https://www.nasa.gov/isru`.

[2] Jahn, R. G., *Physics of Electric Propulsion*, McGraw-Hill Book Company, New York, 1968.

[3] Spence, B., White, S., Wilder, N., Gregory, T., Douglas, M., Takeda, R., Mardesich, N., Peterson, T., Hillard, B., Sharps, P., and Fatemi, N., "Next Generation UltraFlex Solar Array for NASAs New Millennium Program Space Technology 8," *2005 IEEE Aerospace Conference*, 2005, pp. 824–836.

[4] Blevin, H. A., and Thonemann, P. C., "Plasma confinement using an alternating magnetic field," *Nuclear Fusion Supplement, Part 1*, 1962, p. 55.

[5] Kirtley, D., Pancotti, A., Slough, J., and Pihl, C., "Steady operation of an FRC thruster on Martian atmosphere and liquid water propellants," *48th AIAA/ASME/SAE/ASEE Joint Propulsion Conference & Exhibit*, 2012, p. 4071.

[6] Hill, C. S., "Preliminary Results on an Annular Field Reversed Configuration Translation Experiment," *IEPC-2011-281*, 2011.

[7] Brown, D. L., Beal, B. E., and Haas, J. M., "Air Force Research Laboratory high power electric propulsion technology development," *2010 IEEE Aerospace Conference*, 2010, pp. 1–9.

[8] Koelfgen, S., Hawk, C., Eskridge, R., Lee, M., Martin, A., and Smith, J., "A plasmoid thruster for space propulsion," *39th AIAA/ASME/SAE/ASEE Joint Propulsion Conference and Exhibit*, 2003, p. 4992.

[9] Slough, J., Blair, A., Pihl, C., and Votroubek, G., "Magnetically Accelerated Plasmoid (MAP) Thruster - Initial Results and Future Plans," *IEPC-2007-16*, 2007.

[10] Slough, J., Kirtley, D., and Weber, T., "Pulsed plasmoid propulsion: The ELF thruster," *31th International Electric Propulsion Conference*, 2009, pp. 20–24.

[11] Weber, T. E., "The Electrodeless Lorentz Force Thruster Experiment," Ph.D. thesis, University of Washington, 2010.

[12] Woods, J. M., Sercel, C. L., Gill, T. M., Viges, E., and Jorns, B. A., "Data-Driven Approach to Modeling and Development of a 30 kW Field-reversed Configuration Thruster," 2019.

[13] Sercel, C., Woods, J., Gill, T., Viges, E., Van Zanten, R., and Jorns, B., "Design of a 30 kW RMF-FRC," *Poster Presented at the 36th IEPC in Vienna, Austria*, 2019.

[14] Waldock, J., Kirtley, D., and Slough, J., "Electromagnetic optimization of FRC-based pulsed plasma thrusters," *Proc. 33rd Int. Electric Propulsion Conf.(Washington, DC)*, 2013.

[15] Myers, C., Edwards, M., Berlinger, B., Brooks, A., and Cohen, S., "Passive Superconducting Flux Conservers For Rotating Magnetic Field Driven Field Reversed Configurations," *Fusion Science and Technology*, Vol. 61, 2012, pp. 86–103.

[16] Mikellides, P. G., and Neilly, C., "Pulsed INductive Thruster, Part 1: Modeling, Validation, and Performance Analysis," *AIAA 2004-4091, 40th Joint Propulsion Conference and Exhibit*, Fort Lauderdale, Florida, 2004.

[17] Martin, A., and Eskridge, R., "Electrical coupling efficiency of inductive plasma accelerators," 2005. https://doi.org/10.1088/0022-3727/38/23/005.